Exp Brain Res (2001) 136:1–18
DOI 10.1007/s002210000533

RESEARCH ARTICLE

Takao Imai · Steven T. Moore · Theodore Raphan
Bernard Cohen

Interaction of the body, head, and eyes during walking and turning

Received: 5 January 2000 / Accepted: 11 July 2000 / Published online: 14 November 2000

Abstract Body, head, and eye movements were measured in five subjects during straight walking and while turning corners. The purpose was to determine how well the head and eyes followed the linear trajectory of the body in space and whether head orientation followed changes in the gravito-inertial acceleration vector (GIA). Head and body movements were measured with a video-based motion analysis system and horizontal, vertical, and torsional eye movements with video-oculography. During straight walking, there was lateral body motion at the stride frequency, which was at half the frequency of stepping. The GIA oscillated about the direction of heading, according to the acceleration and deceleration associated with heel strike and toe flexion, and the body yawed in concert with stepping. Despite the linear and rotatory motions of the head and body, the head pointed along the forward motion of the body during straight walking. The head pitch/roll component appeared to compensate for vertical and horizontal acceleration of the head rather than orienting to the tilt of the GIA or anticipating it. When turning corners, subjects walked on a 50-cm radius over two steps or on a 200-cm radius in five to seven steps. Maximum centripetal accelerations in sharp turns were ca.0.4 *g*, which tilted the GIA ca.21° with regard to the heading. This was anticipated by a roll tilt of the head of up to 8°. The eyes rolled 1–1.5° and moved down into the direction of linear acceleration during the tilts of the GIA. Yaw head deviations moved smoothly through the turn, anticipating the shift in lateral body trajectory by as much as 25°. The trunk did not anticipate the change in trajectory. Thus, in contrast to straight walking, the tilt axes of the head and the GIA tended to align during turns. Gaze was stable in space during the slow phases and jumped forward in saccades along the trajectory, leading it by larger angles when the angular velocity of turning was greater. The anticipatory roll head movements during turning are likely to be utilized to overcome inertial forces that would destabilize balance during turning. The data show that compensatory eye, head, and body movements stabilize gaze during straight walking, while orienting mechanisms direct the eyes, head, and body to tilts of the GIA in space during turning.

Keywords Locomotion · Trajectory following · Head orientation · Eye orientation · VOR

S.T. Moore · T. Raphan (✉)
Department of Computer and Information Science,
Brooklyn College of CUNY, 2900 Bedford Avenue,
Brooklyn, NY 11210, USA
e-mail: raphan@nsi.brooklyn.cuny.edu
Tel.: +1-718-9514193, Fax: +1-718-9514489

T. Imai · S.T. Moore · T. Raphan · B. Cohen
Department of Neurology, Mount Sinai School of Medicine,
New York, NY, USA

B. Cohen
Department of Physiology and Biophysics,
Mount Sinai School of Medicine, New York, NY, USA

Introduction

Locomotion is associated with coordinated limb, body, head, and ocular movements (Crane and Demer 1997; Hirasaki et al. 1999; Inman 1966; Inman et al. 1981; Maurer et al. 1997; Mergner and Rosemeier 1998; Moore et al. 1999; Winter et al. 1993). Quantitative results about the body, head, and eyes during walking have largely come from two-dimensional studies on linear overground and treadmill locomotion. These studies have shown that the body, head, and eyes rotate in response to the up-down and side-to-side motion to maintain stable head pointing and gaze in space (Crane and Demer 1997; Hirasaki et al. 1999; Moore et al. 1999; Pozzo et al. 1991). Grasso et al. (1996, 1998) studied horizontal head and eye movements during circular walking. They showed that there was anticipatory control of the horizontal head direction so that the head led the trajectory motion in the horizontal plane by up to 20°. There was also horizontal ocular nystagmus with quick phases that moved the eyes and gaze ahead of the body heading, steering the turn (Grasso et al. 1998).

Torsional and vertical head and eye movements were not studied during either linear or circular locomotion and relatively little is known about the underlying mechanisms that coordinate movements of the upper body, head, and eyes in three dimensions during either straight walking or turning. One reason for the lack of information is that there are complex relative rotations and translations between the body, head, and eyes which are not easily related to each other or to the gait trajectory. This complicates both the representational schemes for describing the kinematics of the relative motions of the body, head, and eyes and their quantification. One purpose of this study was to provide such a three-dimensional representational scheme.

During straight walking, there is a characteristic monotonic relationship between stride length and walking speed for velocities ranging from 1.2–1.8 m/s (Andriacchi et al. 1977; Cappozzo 1981; Hirasaki et al. 1999; Murray et al. 1966). Over this range of walking velocities, there is both translation and rotation of the head in the sagittal plane, reaching translational frequencies close to 2 Hz, peak vertical linear accelerations of 0.3–0.5 *g*, and peak pitch velocities of 15–22°/s (Hirasaki et al. 1999; Moore et al. 1999). The magnitude and frequency of the pitch angular and vertical translational head movements are sufficient to activate both the angular and linear vestibuloocular (aVOR and lVOR) and vestibulocollic (aVCR and lVCR) reflexes (Paige 1989; Takahashi 1990), which may play important roles in directing gaze and in stabilizing gait. In support of this, unilateral vestibular disease is associated with instability of gait (Grossman and Leigh 1990; Ito et al. 1995), and astronauts, whose vestibular function has been adapted to microgravity, also experience difficulty when walking a curved path after flight (Bloomberg et al. 1997; Clement and Reschke 1996). Another purpose of this study was to infer a possible role for the vestibular system in producing head and eye movements in three dimensions as the body moves in space.

VOR responses can be characterized as being either compensatory or orienting (Raphan and Cohen 1996; Raphan et al. 1996; Wearne et al. 1999). The high frequency aVOR and lVOR are examples of compensatory responses. The aVOR compensates by producing angular eye velocity that opposes angular head velocity. The lVOR compensates by rotating the eyes to maintain gaze on specific space-fixed targets when subjects are translated laterally or vertically with the head fixed (Paige and Tomko 1991; Schwarz and Miles 1991). Orienting responses tend to align the eyes or the axis of eye velocity with the sum of linear accelerations acting on the head (gravito-inertial acceleration, GIA). Examples of lVOR orienting responses are ocular counterrolling (Miller 1962) and the alignment of the axis of vestibular or optokinetically induced eye velocity to the GIA (Dai et al. 1991; Raphan and Cohen 1996; Raphan and Sturm 1991; Wearne et al. 1999).

The concepts of compensatory and orienting responses developed for the VOR with the head fixed can be generalized to describe movements of the head and eyes during locomotion. The compensatory aVOR has been inferred to stabilize horizontal and vertical fixation of far targets during straight walking (Moore et al. 1999) and to compensate for yaw head movements during circular locomotion (Grasso et al. 1998). The aVCR appears to compensate for pitch body rotation when walking at low velocities (Hirasaki et al. 1999). Compensatory lVCR/lVOR responses would be induced by linear translations that rotate the head and/or eyes to maintain an invariant point relative to the subject's forward motion. Compensatory responses have been observed in vertical head and eye movements that stabilize the head and gaze during linear treadmill locomotion at optimal walking velocities. These head movements maintain an approximate fixed point at the intersection of all head pointing directions in the sagittal plane over the gait cycle (Hirasaki et al. 1999; Moore et al. 1999; Pozzo et al. 1990). An invariant point of head fixation is presumably present during overground walking but has not been systematically studied. Orienting responses during locomotion would tend to align the yaw axes of the head and eyes, which are normally along the spatial vertical when standing, with the tilted GIA. During straight walking and turning, there are significant linear accelerations that produce dynamic tilts of the GIA (Imai et al. 1998). The extent to which these tilts of the GIA induce orienting head, eye, and body movements is not known.

In this study, we present a novel representational scheme for describing the linear and angular motions of the body, head, and eyes to analyze roll, pitch, and yaw of the body, head, and eyes relative to any arbitrary coordinate frame, which translates and rotates in space. The scheme is based on the theory of finite rotations (Goldstein 1980) and the representation of these rotations by axis-angle (Altmann 1986; Raphan 1998; Rodriguez 1840). Utilizing this, we have determined how the body, head, and eyes compensate and orient to variations in the GIA during the locomotion trajectory to maintain stable posture and gaze in three-dimensional space.

Materials and methods

Five normal healthy subjects (four males and one female) were used in this study. Their mean age was 29 years old (27–33 years old), and their mean height was 168 cm (160–174 cm). They had no history of vestibular disease or other disorders that would affect their normal locomotor performance. The experiments were approved by the Institutional Review Board and have been performed in accordance with the ethical standards laid down in the 1964 Declaration of Helsinki. All subjects gave their informed consent prior to their inclusion in the study.

Testing protocol

Subjects were instructed to walk along a straight line for 3 m, turn 90° along a 50- or 200-cm radius to the right, then continue walking along a straight line for 3 m. The trajectory was outlined on the floor with tape, and large objects (cardboard boxes) were placed on the floor approximately 35 cm either side of the trajec-

tory to guide subjects along a uniform path. Subjects were given two training sessions before the data were acquired. First, they walked while looking at the trajectory on the floor. Next, they were instructed to follow the trajectory while looking straight ahead, without touching the laterally placed objects. Following the training sessions, subjects were instructed to walk at a "normal" or "slow" velocity, which were individually determined. Data were acquired from three trials at each of these two walking velocities. The normal walking velocity ranged from 1.4–1.8 m/s, which has previously been shown to be within an optimal range for coordination of head and body movements during locomotion (Hirasaki et al. 1999). We will also refer to this as "moderate walking". Slow walking velocity was less than 1.2 m/s. Linear locomotion was also studied over a straight 8-m path at an optimal walking velocity.

Data acquisition

Data of body and head movements were obtained from a video-based motion analysis system (Optotrak 3020; Northern Digital, Canada) at a rate of 100 Hz. The body coordinate frame was defined by four infrared (IR) markers (diameter 8 mm, weight 5 g) attached to a rectangular plate (75×100 mm) that was securely fixed between the subject's shoulders. This represented the position of the body (trunk) in space, i.e., the upper part of the trunk above the hips. Head movement was obtained by tracking the three-dimensional position of six IR markers attached to a lightweight (120 g) headband. The raw position data was processed after testing to yield Euler angles (yaw, pitch, and roll) and three-dimensional translation coordinates of rigid body models of the head and body formed from the IR marker data. The angular accuracy and resolution of the Optotrak system is 0.1° in yaw, pitch, and roll at a distance of 4 m from the sensor (Hirasaki et al. 1999), and the translational accuracy is 0.1 mm at a distance of 4.0 m from the sensor (manufacturer's specifications).

Eye movements were recorded from the subject's left eye at a sampling rate of 60 Hz using a video pupil tracker (ISCAN, Cambridge, Mass., USA). The subject's eye was imaged with a miniature video camera (EYECAM; ISCAN), mounted on lightweight goggles (114 g). The goggles fit the eye sockets tightly, and there was negligible camera movement relative to the head (Moore et al. 1999). The eye was illuminated by a single 940-nm IR LED, and the image of the eye was reflected onto the camera CCD by an IR-sensitive "hot" mirror, which was transparent to light in the visible frequency range. This allowed the subjects a clear field of view.

The raw body and head translation data were filtered using a 3-point median (to remove single-point spikes) followed by a 7-point moving average filter. This filter combination did not affect the phase of the original waveform. This has been confirmed experimentally by cross-correlation of the original raw waveform with the filtered data (Moore et al. 1999). This filter had a gain of –3 dB at 10 Hz and a null gain at 18 Hz. Body and head velocities were calculated by differentiation of the filtered position waveforms with a 2-point forward difference algorithm. Body acceleration was calculated by applying the 2-point forward difference algorithm to the velocity waveform. The filter bandwidths were similar to those used in previous locomotion studies (Bloomberg et al. 1997; Crane and Demer 1997; Moore et al. 1999). The gain and phase characteristics of the filters were determined from the input-output relationship of sinusoidal waveforms from 0.1–30 Hz.

Coordinate frames

Coordinate frames that describe the motion of the body, head, and eyes while moving through space were defined in a hierarchical fashion (Fig. 1A). The primary coordinate frame was the spatial or inertial frame (X_S, Y_S, Z_S) of the body relative to space. We also defined coordinate frames for the body (X_B, Y_B, Z_B), head (X_H, Y_H, Z_H), and eye (X_e, Y_e, Z_e). The body coordinate frame has alternatively been referred to as the trunk coordinate frame (Hirasaki et al. 1999). The orientation of each frame in space can be described by a transformation from the space-fixed coordinates to each of the other frames. We also defined a body trajectory frame (X_T, Y_T, Z_T), which described where the body was heading at any point in time.

Spatial, body, and head coordinate frames

The inertial space-fixed coordinate frame (X_S, Y_S, Z_S) was defined using a calibration jig comprised of three IR markers which defined the origin and the X_S-Z_S plane. The Z_S-axis was parallel to the spatial vertical (positive upward), and the positive X_S-axis was parallel to the direction of straight walking before turning and orthogonal to Z_S. The Y_S-axis was positive to the subject's left and orthogonal to the X_S-Z_S plane (Fig. 1A). The head and body coordinate frames were defined in a similar manner from the IR markers of the head and trunk rigid bodies, respectively (Hirasaki et al. 1999; Moore et al. 1999). A body-fixed coordinate frame (X_B, Y_B, Z_B) was defined as X_B parallel to the dorsoventral axis (positive forward), Y_B parallel to the transverse axis (positive to the subject's left), and Z_B normal to the X_B-Y_B plane (positive upwards). The head-fixed coordinate frame (X_H, Y_H, Z_H) was defined such that the roll axis, X_H, was parallel to the nasooccipital axis (positive forward), the pitch axis, Y_H, was parallel to the interaural axis (positive left), and the yaw axis, Z_H, was normal to the X_H-Y_H plane (positive upwards). The eye-fixed coordinate frame (X_e, Y_e, Z_e) was defined with the origin at the center of the eye and X_e passing through the center of the pupil (positive forward) and normal to Y_e-Z_e plane. The orientation of the eye coordinate axes relative to the head can be given by a rotation matrix and has been specified by three Euler angles (Fick 1854; Goldstein 1980), rotation vectors, and quaternions (Haustein 1989; Tweed et al. 1990), or by axis-angle or Euler-Rodriguez parameters (Altmann 1986; Raphan 1998; Rodriguez 1840; Schnabolk and Raphan 1994; Tweed et al. 1994). Horizontal, vertical, and torsional eye movements were measured in the head-fixed frame (X_H, Y_H, Z_H).

In this study, we considered the rotations and translations of the head and body in space as rigid bodies. The Optotrak software determined these rotations and translations. The origin of the body frame was at the center of a four LED rigid body, which was securely placed on the subject's shoulder and the origin of the head coordinate frame was located at the center of the head band. The origin of the spatial frame was some point at the center of the room. The linear position of the body relative to the spatial frame is only considered in Fig. 4A, B, which are top down views of the linear motion of the body origin in this two-dimensional projection. The velocity of the body in this projected plane is the direction of heading, which is used to define the trajectory coordinate frame. The origin of this coordinate frame changes with time as the body translates in this two-dimensional space, but its Z-axis is always parallel to the spatial Z-axis. All other transformations which were considered in this report are related to the relative rotations of the body, head, and eyes. These rotations are independent of the origin of the coordinates to which they are referenced.

Trajectory coordinate frame

During walking, the body follows a trajectory in the X_S-Y_S plane, which can be determined by the linear motion of a point on the body (x_S,y_S,0). To study the movement of the body in space we defined a trajectory coordinate frame (X_T, Y_T, Z_T), with the origin at (x_S,y_S,0). The linear velocity of the body at each point of the trajectory determined the X_T-axis of the trajectory coordinate frame, which was parallel to the direction of forward linear motion. This was defined as the heading. The axis orthogonal to the heading, but lying parallel to the X_S-Y_S plane was Y_T. The Z_T-axis was parallel to the spatial vertical, Z_S (Fig. 1B). The orientation of this trajectory coordinate frame could be given by its rotation with respect to the space-fixed coordinate frame (Fig. 1A) and could be

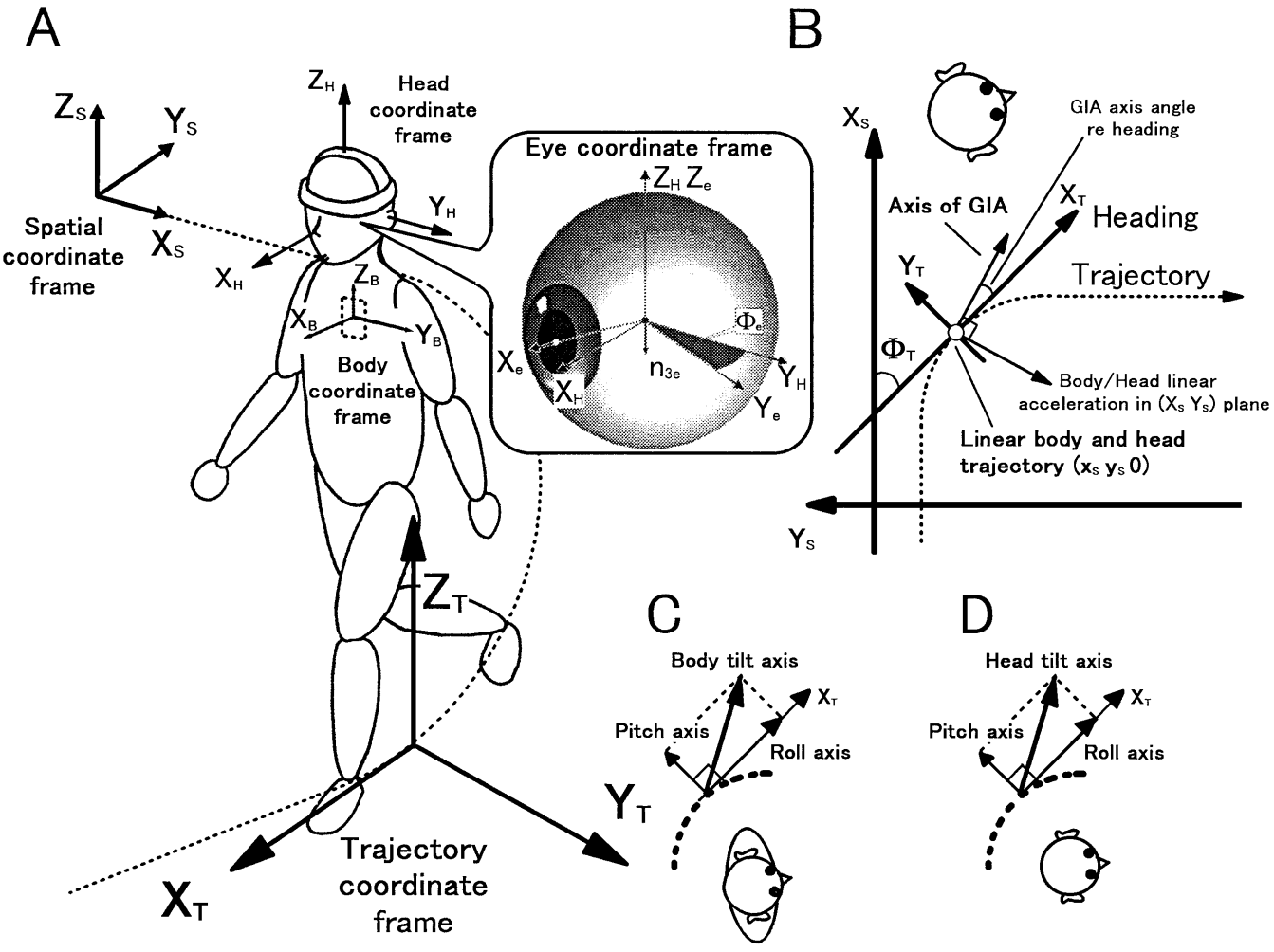

Fig. 1A–D Coordinate frames for describing the motion of the body, head, and eyes during locomotion. **A** The spatial coordinate frame (X_S, Y_S, Z_S) is fixed relative to space. The body coordinate frame (X_B, Y_B, Z_B) moves linearly and rotates relative to the spatial coordinate frame. The head coordinate frame (X_H, Y_H, Z_H) rotates relative the body frame. The eye coordinate frame (X_e, Y_e, Z_e) rotates relative to the head. **B** The trajectory is defined as the path that the origin of the body coordinate frame follows during locomotion in a plane parallel to the spatial horizontal plane. The heading is defined as the direction of the forward velocity and is tangent to the trajectory at each point (x_S, y_S, 0). The heading is taken as the X_T coordinate axis of the trajectory coordinate frame. Y_T is perpendicular to this axis and lies in the X_S-Y_S plane. The Z-axes of the trajectory and spatial frames are parallel. The angle, Φ_T, is the yaw orientation of the heading relative to space and is referred to as the heading direction or just heading. The body linear acceleration during turning gives rise to a centripetal acceleration in the X_S-Y_S plane, which sums with the acceleration of gravity to give a rotation of the gravito-inertial acceleration (GIA) about the axis of the GIA. **C** The tilt of the body gives rise to pitch and roll components, which are along the X_T- and Y_T-axes, respectively. **D** Head tilt can similarly be related to the trajectory component (roll) and an orthogonal component (pitch)

specified by an axis-angle (Raphan1998). The axis of rotation was parallel to the Z_S-axis and the angle, Φ_T, was determined by the orientation of X_T relative to X_S, given as follows (Fig. 1B):

$$\Phi_T = Tan^{-1}\frac{\dot{y}_S}{\dot{x}_S} \tag{1}$$

The angle Φ_T (Fig. 1B) defines the heading of the body in space at any point on the trajectory (x_S, y_S, 0), and the dot indicates the respective derivatives of x_S and y_S. Using a right-handed convention and a view from the top of the head, the linear head velocity component along the Y_S-axis will be negative for right turns and the angle Φ_T will be negative. For left turns, the linear velocity along the Y_S-axis will be positive and Φ_T will be positive. The rotation of the trajectory frame relative to the spatial frame can be given by a rotation matrix, R_T, as:

$$R_T = \begin{bmatrix} \cos\Phi_T & -\sin\Phi_T & 0 \\ \sin\Phi_T & \cos\Phi_T & 0 \\ 0 & 0 & 1 \end{bmatrix} \tag{2}$$

This matrix also transforms vectors in the trajectory coordinate frame to the spatial frame. Therefore, a matrix which transforms vectors in the spatial frame to the trajectory coordinate frame is the inverse of this matrix, R_T^{-1}, given by its transpose (Goldstein 1980):

$$R_T^{-1} = \begin{bmatrix} \cos\Phi_T & \sin\Phi_T & 0 \\ -\sin\Phi_T & \cos\Phi_T & 0 \\ 0 & 0 & 1 \end{bmatrix} \tag{3}$$

That is, any vector in space coordinates can be converted to trajectory coordinates through multiplication by the matrix given by Eq. 3.

Representations of GIA tilts in trajectory coordinates

The GIA changes orientation from the spatial vertical while moving along the trajectory due to linear acceleration of the body. The

GIA vector can be described as a rotation whose axis lies in the X_T-Y_T plane. The axis-angle can be determined as a rotation of the GIA relative to a unit vector along the Z_T-axis. The GIA vector at any given point in the trajectory can be given in space-fixed coordinates as:

$$GIA_S = \begin{bmatrix} \ddot{x}_S \\ \ddot{y}_S \\ \ddot{z}_S + a_g \end{bmatrix} \quad (4)$$

where GIA_S is the GIA vector, $\ddot{x}_S$, $\ddot{y}_S$ and $\ddot{z}_S$ are the linear acceleration of the body, and a_g is the acceleration of gravity specified in the inertial space-fixed coordinate system. This vector can be given in the trajectory coordinate frame by mapping the vector using the matrix given in Eq. 3. This vector is given by:

$$GIA_T = \begin{bmatrix} \ddot{x}_S \cos\Phi_T + \ddot{y}_S \sin\Phi_T \\ \ddot{x}_S \sin\Phi_T + \ddot{y}_S \cos\Phi_T \\ \ddot{z}_S + a_g \end{bmatrix} \quad (5)$$

The axis of GIA_T tilt in the trajectory coordinate frame can then be obtained as a unit vector along the direction of the cross product,

$$\hat{n}_{GIA} = \frac{\hat{a}_z \wedge GIA_T}{\|GIA_T\| \sin\Phi_G} \quad (6)$$

where a_z is a unit vector along the Z_T-axis, $\wedge$ represents the cross product, $\| \|$ represents the norm of the vector, $\hat{n}_{GIA}$ is the axis of the GIA tilt which lies in the X_T-Y_T plane, and Φ_G is the angle of the GIA. This vector can be given as:

$$\hat{n}_{GIA} = \frac{\begin{bmatrix} \ddot{x}_S \sin\Phi_T + \ddot{y}_S \cos\Phi_T \\ \ddot{x}_S \cos\Phi_T + \ddot{y}_S \sin\Phi_T \\ 0 \end{bmatrix}}{\sqrt{\ddot{x}_S^2 + \ddot{y}_S^2}} \quad (7)$$

The angle of the GIA tilt, Φ_G is:

$$\Phi_G = Tan^{-1}\left(\frac{\sqrt{\ddot{x}_S^2 + \ddot{y}_S^2}}{a_g + \ddot{z}_S} \right) \quad (8)$$

Thus, the representation of the rotation in axis-angle form is $\Phi_G \hat{n}_{GIA}$ (Goldstein 1980; Raphan 1998), where $\hat{n}_{GIA} = (n_{1GIA}, \hat{n}_{2GIA}, 0)$ represents the GIA tilt in the trajectory coordinate frame.

Computation of body and head orientation in three dimensions

The body coordinate frame, in addition to translating with the body, rotates relative to the trajectory coordinate frame (Fig. 1A, C). The rotation matrix, R_{BS}, represents the rotation of the body in the spatial frame, and R_{BT} represents the rotation matrix of the body relative to the trajectory frame, obtained using Eq. 3 as follows:

$$R_{BT} = R_T^{-1} R_{BS} \quad (9)$$

The orientation of the head coordinate frame relative to space is represented by the rotation matrix R_{HS}. The rotation of the head relative to the trajectory coordinate frame, R_{HT}, is obtained using Eq. 3.

$$R_{HT} = R_T^{-1} R_{HS} \quad (10)$$

The axis-angle representation of the body and head orientation relative to either the space or trajectory coordinate frames could then be extracted from the associated matrix (i.e., R_{BS}, R_{BT}, R_{HS}, R_{HT}) using the Euler-Rodriguez formula (Goldstein 1980).

$$\begin{bmatrix} n_1 \\ n_2 \\ n_3 \end{bmatrix} = \frac{1}{2\sin\Phi} \begin{bmatrix} r_{32} - r_{23} \\ r_{13} - r_{31} \\ r_{21} - r_{12} \end{bmatrix} \quad (11)$$

$$\Phi = \cos^{-1}\left(\frac{Tr R - 1}{2} \right) \quad (12)$$

where r_{ij} is the element in the ith row and jth column of the relevant matrix, R, and *Tr* is the trace operator. The corresponding roll, pitch, and yaw components of the body rotation relative to the trajectory coordinate frame at each instance of time were given as:

$$[n_{1BT}\Phi_{BT}, n_{2BT}\Phi_{BT}, n_{3BT}\Phi_{BT}], \quad (13)$$

and the head relative to trajectory coordinates can similarly be given as:

$$[n_{1HT}\Phi_{HT}, n_{2HT}\Phi_{HT}, n_{3HT}\Phi_{HT}] \quad (14)$$

The body and head axis-angle orientation can also be computed relative to space coordinates ($\Phi_{BS}\hat{n}_{BS}$ and $\Phi_{HS}\hat{n}_{HS}$) from the matrices R_{BS} and R_{HS}, respectively, using Eqs. 11 and 12. The unit vectors $\hat{n}_{BS}$ and $\hat{n}_{HS}$ are the body and head orientation axes, with corresponding angles Φ_{BS} and Φ_{HS}. To determine the orientation parameters for the head relative to the body, Eqs. 11 and 12 can be applied to the matrix,

$$R_{HB} = R_{BS}^{-1} R_{HS} \quad (15)$$

Relative tilts of the body and head in a variety of coordinate frames could then be compared with the orientation of the GIA. If, for example, the GIA tilts about an axis which is coincident with the trajectory heading, X_T, then n_{2GIA} would be zero. If the axis component of head tilt, n_{2H}, equals zero, it would indicate that the head is tilted about an axis coincident with the GIA tilt. In both instances, the direction cosines of the axis of GIA and head tilt would indicate that the axes were along the trajectory heading.

Translation due to the pitch rotation of the trunk could add to the computation of the vertical translation of the body coordinate frame in space. We calculated the body pitch rotation axis using the instantaneous rotation axis technique (Moore et al. 1997), and found it to be located at the third lumbar vertebra (L3) at the level of the hips. The maximum pitch of the body during walking was always less than 2°. If it is assumed that stride length is approximately 150 cm and that the distance from the body pitch axis and the body coordinate frame is 30 cm, then the amount of translation due to the rotation of the body would be less than 0.7% (30*tan(2°)/150*100). The translation of the body coordinate frame due to its eccentric location relative to the body pitch axis was therefore negligible, and was not considered when calculating the trajectory of the body in the spatial horizontal (X_S-Y_S) plane.

Stride and turn averaging

Stride averaging was used to normalize body and head position waveforms across subjects during both linear walking and turning. For straight walking, the time scale was stretched or contracted for each trial so that it represented an average stride length. Each 15-s epoch was subdivided into strides using the local minima of the heel vertical position (left heel strike). Each stride waveform was resampled to provide 100 equally spaced data points following a cubic spline interpolation, and an average stride waveform calculated from these individual strides (Moore et al. 1999). For turning, the time scale for each trial was stretched or contracted to represent an average 90° turn, consistent with the average number of steps for that turning radius and walking velocity. Since the number of strides for making the 90° turns were dependent on the turning radius, the data could not be normalized with respect to stride length, but were rather normalized with respect to the degree of turn. The right heel strike closest to the beginning of each turn was used to designate and align the beginning of the turn for all trials. Beginnings and ends of turns were determined from the yaw body trajectory. The data from beginning to the end of each 90°-turn trial were then resampled to provide 100 equally spaced data points, which were interpolated using a cubic spline fit as for the straight walking. The abscissa designated the percentage of the average 90° turn. The average number of steps for all subjects for completing the turn at each turning radius was determined and recorded on the figure. All subjects used two steps for all trials for 50-cm turns. To make 200-cm turns, the average was six steps, ranging from five to seven steps.

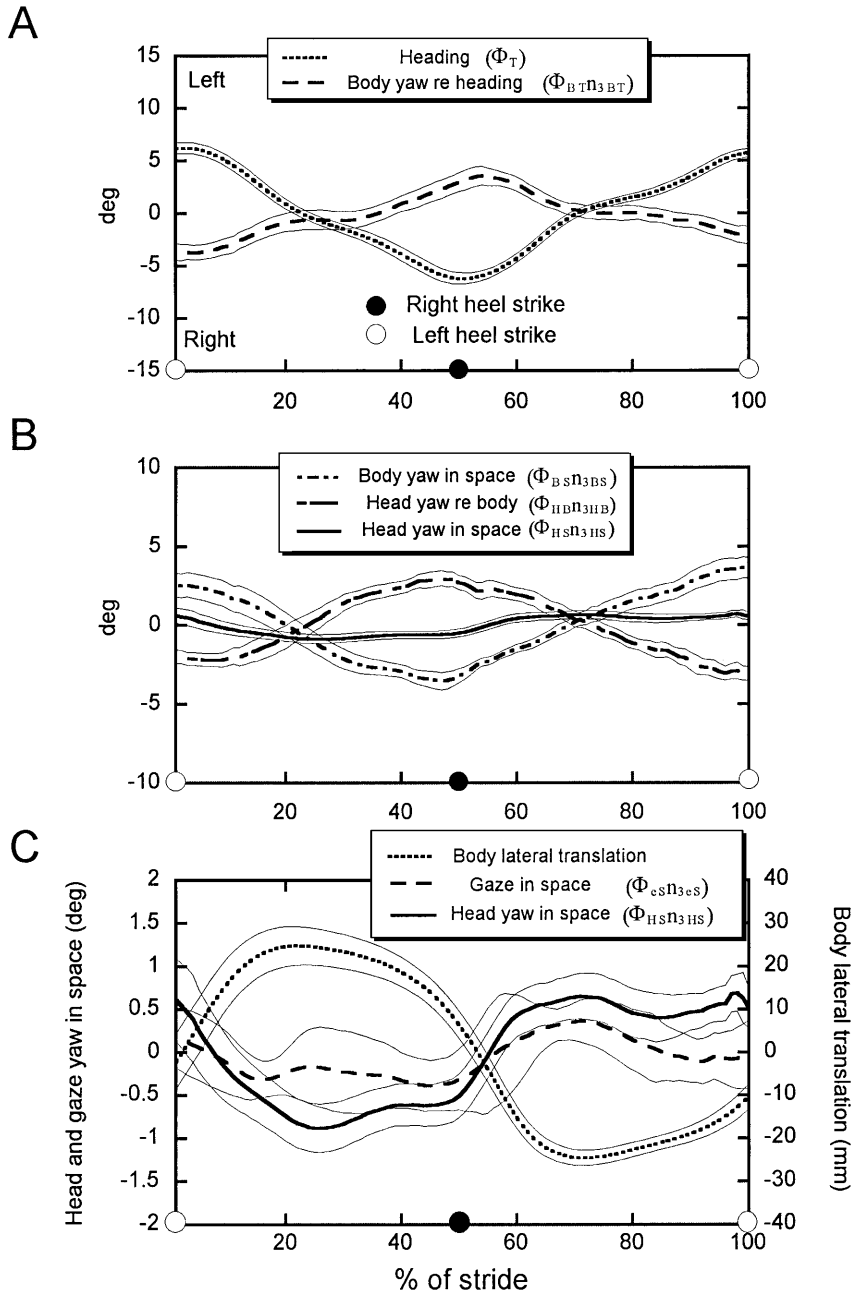

Fig. 2A–C Averaged stride data for five subjects, three trials per subject, while walking a straight path. The *abscissa* shows one average stride length, with the heel strikes for the right (●) and left (○) feet, respectively. This notation is utilized in all relevant legends. **A** Heading (Φ_T) and body yaw re heading ($\Phi_{BT}n_{3BT}$). The trajectory was approximately sinusoidal, with peak amplitude of about 6°. There was also sinusoidal yaw of the body, which was opposite to the heading with peak amplitude of 3–4°. **B** Head yaw in space ($\Phi_{HS}n_{3HS}$), body yaw in space ($\Phi_{BS}n_{3BS}$), and head yaw re body ($\Phi_{HB}n_{3HB}$). Head yaw relative to the body was compensatory for the body yaw in space. Consequently, the yaw of the head in space was small, and it tended to maintain the nasooccipital axis of the head aligned with the forward direction of locomotion. **C** Head yaw in space ($\Phi_{HS}n_{3HS}$), gaze yaw in space ($\Phi_{eS}n_{3eS}$), and lateral body translation. Although head yaw in space was compensatory for the lateral translation of the body, gaze yaw in space was smaller, indicating additional ocular compensation for the lateral translation of the body

Computation of eye orientation in three dimensions

Three-dimensional eye position relative to the head was calculated from video images of the left eye and represented in axis-angle form. Pitch and yaw eye movements were measured using a video-based pupil tracker (ISCAN). Horizontal ($n_3\Phi_e$) and vertical ($n_2\Phi_e$) eye position relative to the head (Fig. 1A, inset) were computed from the raw pupil data using a calibration file acquired prior to testing (Moore et al. 1999). The subject was seated and asked to fixate on horizontal and vertical targets at gaze angles of 2.86° and 5.71° on a calibration grid placed 2 m distant while maintaining the head in a stationary position. The center point of the grid was positioned directly in front of the subject at eye level. Multiple calibrations were performed for each subject and head movement data were analyzed to ensure the validity of the eye position data for the calibration file to be utilized. The torsional component of eye position ($n_1\Phi_e$) was determined from video recordings after testing using an iris landmark tracking technique (Imai et al. 1999).

To determine the orientation parameters of gaze relative to space, Eqs. 11 and 12 can be applied to the matrix,

$$R_{eS} = R_{HS}R_e \quad (16)$$

where R_e represents the rotation matrix of the eye relative to the head coordinate frame.

Results

Yaw, pitch, and roll of the head and body during straight walking

During straight walking the average velocity was 1.6±0.1 m/s, with a corresponding stride frequency of

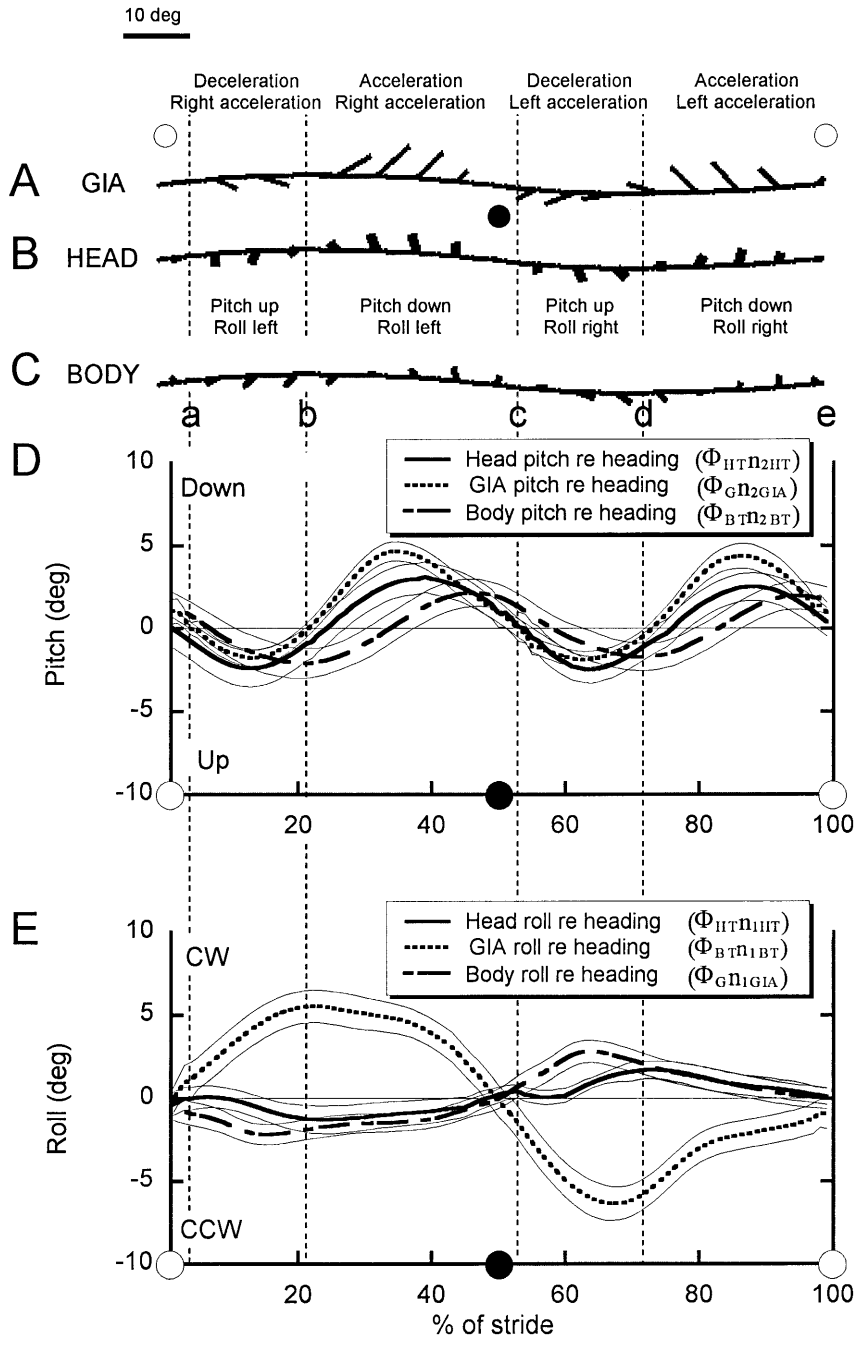

Fig. 3 **A–C** GIA, head, and body tilt axis data from a typical subject while walking a straight path. GIA and head tilt axes were oppositely directed in the forward and backward direction of locomotion, and were same in the right and left direction. This indicates that the head and GIA tilted in the same direction in the pitch plane, but tilted in the opposite direction in the roll plane. The body tilt axis had some delay relative to head tilt axis. **D, E** Averaged stride data for five subjects while walking a straight path. **D** Head pitch re heading ($\Phi_{HT}n_{2HT}$), GIA pitch re heading ($\Phi_{G}n_{2GIA}$), and body pitch re heading ($\Phi_{BT}n_{2BT}$). Head pitch re heading and GIA pitch re heading were in phase, but body tilt re heading had some delay. **E** Head roll re heading ($\Phi_{HT}n_{1HT}$), GIA roll re heading ($\Phi_{G}n_{1GIA}$), and body roll re heading ($\Phi_{BT}n_{1BT}$). Head and body roll were in the same direction, but GIA roll was in the opposite direction

0.95±0.05 Hz. The trajectory was approximately sinusoidal, with a maximal variation in heading (Φ_T) of 6° (Fig. 2A). Head and body yaw movements occurred at a frequency corresponding to the stride frequency. There was sinusoidal yaw of the body, which was opposite to heading, with a relative peak amplitude of 4°. A peak head yaw of 3° relative to the body was compensatory for the peak 3.5° body yaw in space (Fig. 2B). Consequently, head yaw oscillation in space was small (less than 1°), and the nasooccipital axis of the head was close to being aligned with the forward direction of locomotion (Fig. 2B). Although head yaw in space was small, it compensated for the lateral translation of the body and head to stabilize gaze in space (Fig. 2C), in a similar manner as for vertical head movements (Hirasaki et al. 1999; Moore et al. 1999). Compensation was not complete, however, and was further reduced by eye yaw in head, likely produced by activation of the aVOR.

There was also pitch and roll rotation of the body and head relative to the heading. Typically, the body decelerated following heel strike (Fig. 3A *open* and *closed circles*). Immediately after left heel strike early in the first quarter cycle (*first open circle*), the body moved to the left and decelerated in the forward direction. Since acceleration is 180° out of phase with position, the GIA vector tilted back and to the right. Consequently, the GIA axis was oriented

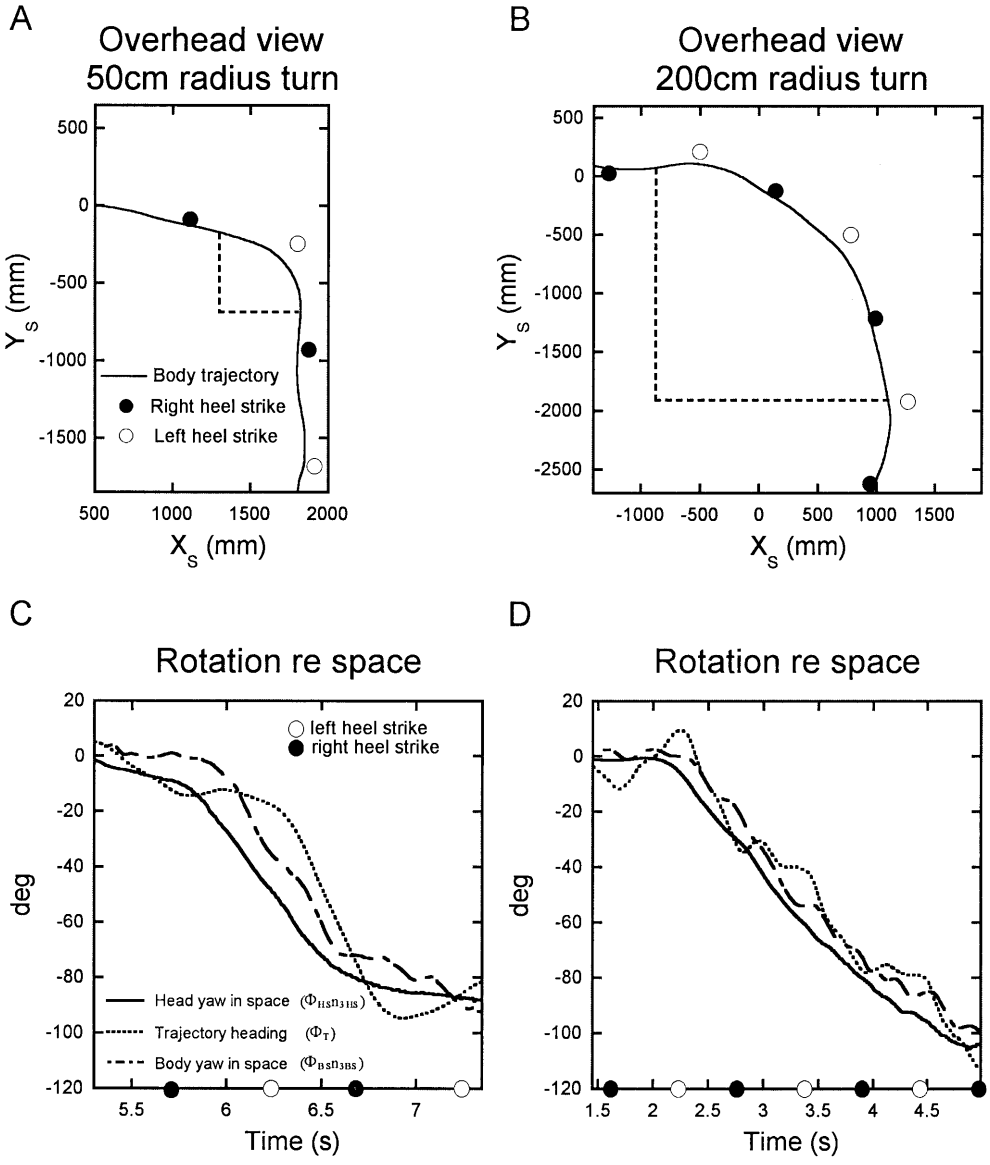

Fig. 4 A, B Heel strikes for right (●) and left (○) feet and the trajectory (–) during (**A**) small-radius and (**B**) large-radius turns. Since the trajectory is shown on the right side of the right heel, it indicates that the head was leaning into the turn. **C, D** Head yaw in space ($\Phi_{HS}n_{3HS}$), body yaw in space ($\Phi_{BS}n_{3BS}$), and trajectory heading (Φ_T) data from a typical subject during a 90° turn to the right over 50-cm radii (**C**) and 200-cm radii (**D**). During turns of both radii, the head steered smoothly around the turn, even though there were oscillatory patterns of the heading and the body yaw in space. The head led the heading direction and body yaw, independent of the turning radius

forward and to the right (Fig. 3A *GIA*). Approximately halfway through the step, the body began to accelerate in the forward direction, and the GIA axis was oriented forward and to the left. Following right heel strike (*closed circle*), the body moved to the right, accelerating to the left and decelerating in the forward direction, which oriented the GIA axis backward and to the right. Midway through the step, the body again accelerated in the forward direction, and the GIA axis pointed back and to the left. The head rotation axis followed the lateral movement of the axis of the GIA, but the forward/backward directions were reversed (Fig. 3B). As a result, the forward/backward movement of the head was aligned with the GIA, but the lateral movement of the head was out of phase with it. The body rotation axis had similar shifts in the axis of rotation as the head, but the shifts were delayed (Fig. 3C). Thus, the directions of lateral tilt of the GIA and head were not coincident, but the head and body moved in the sagittal plane together with the GIA.

Average pitch and roll angles (mean and 95% CI) for tilts of the GIA relative to the heading were computed for the five subjects (Fig. 3D, E). The predominant frequency of head and body pitch rotation was twice the stride frequency. The GIA pitched back following left heel strike in the first 20% of the stride cycle (negative pitch angle), indicating forward-deceleration (Fig. 3D *interval ab*). The GIA also rolled clockwise (Fig. 3E), indicating acceleration to the right. The positive angle of pitch and clockwise roll of the GIA for the next 30% of the cycle represented forward and continued rightward acceleration (Fig. 3D, E *interval bc*). Following right heel strike, there was an approximately symmetrical relationship. That is, there was forward deceleration and leftward acceleration (negative GIA pitch and roll) for the next 20% of the cycle (Fig. 3D, E *interval cd*), followed by forward and leftward acceleration (Fig. 3D, E *interval de*). The GIA tilts about pitch and roll reached maximum values of approximately 5–7° (Fig. 3D, E).

Comparing pitch and roll tilts of the GIA, there was side-to-side acceleration (roll) at one cycle for every two cycles of fore-aft (pitch) acceleration (Fig. 3D, E). The amplitude of pitch head movements (about 3°) was consistent with pitch magnitudes obtained during treadmill walking (Hirasaki et al. 1999; Moore et al. 1999), and was greater than that of roll movements (Fig. 3D, E). Body rotation had a phase lag of approximately 60° in pitch relative to head rotation, but body rotation led the head during roll rotations (Fig. 3D). Body rotation was primarily in the pitch plane, with a magnitude of 3° (Fig. 3E).

Head trajectories and yaw rotation during turning

Trajectories and corresponding yaw body and head rotations were studied during a 90° turn to the right over small (50 cm) and large (200 cm) radii while walking at a moderate (1.5±0.1 m/s) and slow (0.8±0.1 m/s) pace. During small-radius turns, the body moved smoothly along an approximate circular trajectory (Fig. 4A). The subject executed the turn by pivoting on the left foot (Fig. 4A *open circles*), with a corresponding decrease in forward velocity (21.2±7.7%). One subject pivoted on the right foot. During large-radius turns, all subjects pivoted successively on the left foot and maintained a straight trajectory between left heel strikes (Fig. 4B). Generally, it took three pivots to complete the turn, and forward velocity was maintained. During a typical subject trial at 1.5 m/s walking velocity, the head steered smoothly around the turn at both small (50 cm; Fig. 4C) and large (200 cm; Fig. 4D) turning radii, even though there were oscillations in heading and body yaw in space.

In average data for 15 turns from five subjects, the trajectory was smoother for shorter turning radii, regardless of velocity (Fig. 5A, B). For slow walking at the larger turning radius, the trajectory angle had a zero or close-to-zero slope at certain segments (Fig. 5C, D *arrows*). This indicated that angular movement about the heading had ceased for short periods when the outside (left) foot was off the ground. Head yaw in space was maintained smoothly in all cases (Fig. 5A–D *solid lines*), leading the heading by up to 25° (Fig. 5E–H), similar to findings of Grasso et al. (1996). For 50-cm turns, the lead increased over each step length, reaching a peak immediately following the pivot on the left foot (Fig. 5E, F). The lead then decreased over the next step. There was a similar anticipation for larger radii of turning, with peak head yaw occurring at each pivot on the left foot (Fig. 5G, H).

Although head yaw was smooth, body yaw oscillated by about 7° about the heading (Fig. 5I–L). (The subject who pivoted on the right foot had a body oscillation opposite to subjects that pivoted on the left foot; not shown). The magnitude and phase of the body oscillations relative to heel strike closely followed the pattern during straight walking for all subjects (Fig. 2A). Peak body yaw occurred at or slightly after left heel strike (Fig. 5I–L). Thus, by pivoting on the left foot, subjects utilized the natural oscillation of the body during locomotion to facilitate the anticipatory yaw rotation of the head. The single subject who pivoted on the right foot still had a head lead relative to the heading. Body and head yaw were oppositely directed, however, and the head lead relative to heading was smaller than for subjects pivoting on the left foot.

Yaw eye and gaze movements during turning

Eye movements during turning compensated for the yaw axis head movement for both small and large-radius turns. Eye position first shifted in saccades in the direction of the turn, interspersed with slower compensatory eye movements, in some instances reaching yaw angles of 50° relative to the head (Fig. 6A). Eye position relative to the head then returned to zero when the turn was completed. In order to determine the extent of yaw eye deviation relative to the head as a function of turning radius and velocity, yaw eye position was fit by a polynomial and peak eye deviation determined (Fig. 6B). Eye deviation from the mid-position was greatest for smaller radii and higher speeds of walking (Fig. 6C). The eye movements relative to the head resulted in saccadic changes in gaze with a stable gaze position being held in space between the saccadic flicks (Fig. 6D, E). Thus, gaze led the head turn, so that the eyes were directed further into the direction of turning than the head (Fig. 6D, E). This lead was accomplished through saccadic positioning, whereas the aVOR and vision compensated for the smooth turn of the head in space.

Head and body tilts during turning

There was striking alignment of the axes of the head and body with the tilts of the GIA during turning (Fig. 7A). In a typical trial, there was a sustained 8° roll of the head about the heading (X_T-axis) during initial portions of the turn, which then fell to approximately 5° (Fig. 7B). The body rolled a small amount (ca 3°) about the heading when the head roll was maximal. Then body roll decreased in conjunction with the head roll, finally rising to 5° as the head roll declined (Fig. 7B). During small-radius turns (Fig. 7C), small oscillations in head and body pitch were present at ca 2.0 Hz, similar to those found during straight walking. During large-radius turns, head pitch did not increase, although body pitch was larger and more consistent with straight walking. There was an average sustained roll of the head during the execution of the turn, but the head roll was more transient, reaching peaks briefly before dropping back. This suggests that large-radius turns are comprised of quick turns interspersed with straight walking. Prior to and following completion of a turn, the axis-angle of the GIA tilt and corresponding body and head tilts were similar to those described for straight walking (Fig. 7A).

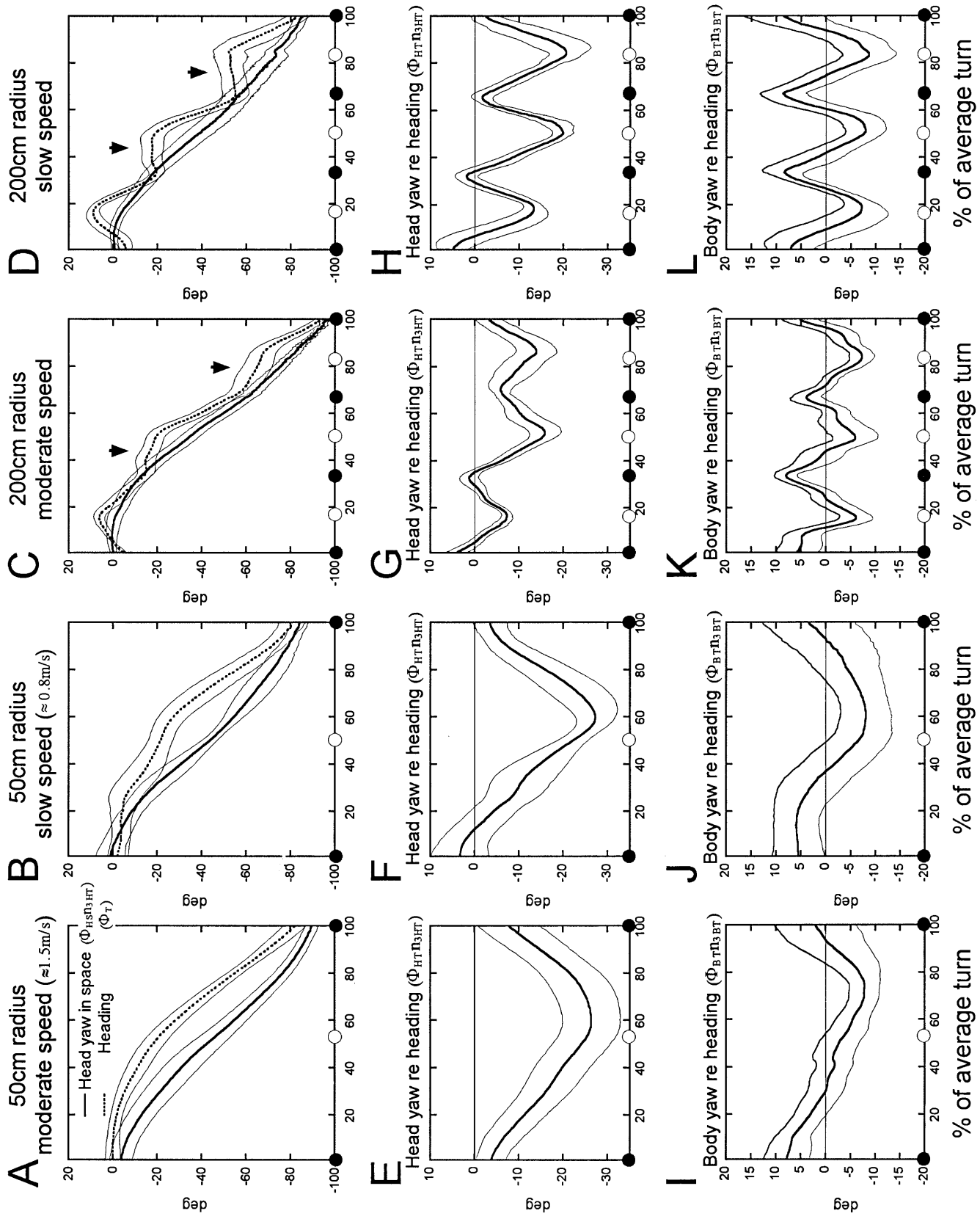
A
50cm radius
moderate speed (≈1.5m/s)
Head yaw in space (Φ_{HSn3HT})
Heading (Φ_T)
B
50cm radius
slow speed (≈0.8m/s)
C
200cm radius
moderate speed
D
200cm radius
slow speed
E
Head yaw re heading (Φ_{HTn3HT})
F
Head yaw re heading (Φ_{HTn3HT})
G
Head yaw re heading (Φ_{HTn3HT})
H
Head yaw re heading (Φ_{HTn3HT})
I
Body yaw re heading (Φ_{BTn3BT})
J
Body yaw re heading (Φ_{BTn3BT})
K
Body yaw re heading (Φ_{BTn3BT})
L
Body yaw re heading (Φ_{BTn3BT})
deg
% of average turn

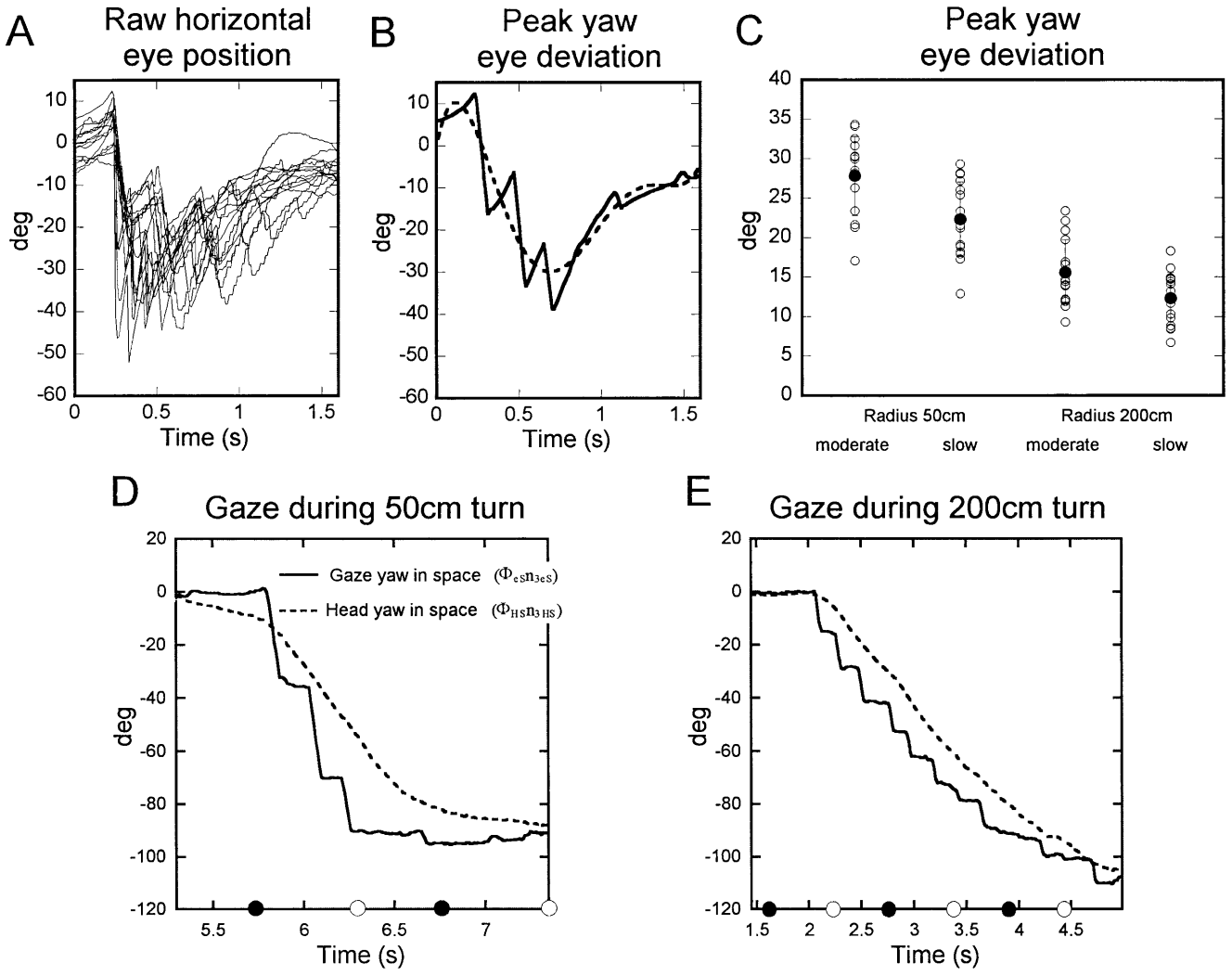

Fig. 6 **A** Yaw eye ($\Phi_e n_{3e}$) data from all trials of all subjects while turning over 50-cm radii at moderate speed. During turning, subjects' eyes deviated to the inside. **B** In order to determine the extent of yaw eye deviation relative to the head as a function of turning radius and velocity, the yaw eye deviation was fit by a polynomial and the peak eye deviation determined. **C** The smaller the radius and the higher the speed of walking, the greater the eye deviation. **D, E** Head yaw in space ($\Phi_{HS}n_{3HS}$) and gaze yaw in space ($\Phi_{eS}n_{3eS}$) data from a typical subject during a 90° turn to the right over 50-cm radii (**D**) and 200-cm radii (**E**). Gaze led the turn and was held stable in space between the saccadic flicks

◀ **Fig. 5A–L** Averaged stride data for five subjects (three trials per subject) while turning. **A–D** Head yaw in space ($\Phi_{HS}n_{3HS}$) and heading (Φ_T) during a 90° turn to the right over a 50-cm radius at moderate speed (**A**), 50-cm radius at slow speed (**B**), 200-cm radius at moderate speed (**C**), and 200-cm radius at slow speed (**D**). Head yaw was smooth at both radii and walking velocities. The trajectory was smoother at the faster walking velocities. For 200-cm radii, at slow walking speeds, the trajectory angle had an approximately zero slope at certain segments in the trajectory (*arrows*). **E–H** Head yaw re heading ($\Phi_{HT}n_{3HT}$) during a 90° turn to the right over a 50-cm radius at moderate speed (**E**), 50-cm radius at slow speed (**F**), 200-cm radius at moderate speed (**G**), and 200-cm radius at slow speed (**H**). There was anticipation with peak head yaw occurring at each pivot on the left foot. **I–L**. Body yaw re heading ($\Phi_{BT}n_{3BT}$) during a 90° turn to the right over a 50-cm radius at moderate speed (**I**), 50-cm radii at slow speed (**J**), 200-cm radii at moderate speed (**K**), and 200-cm radii at slow speed (**L**). The magnitude and phase of the body oscillations relative to heel strike closely followed the pattern during straight walking

The relationship of GIA tilt to head and body tilt for small-radius turns was also present in average data from the five subjects. At the start of the turn (first 20%), the GIA axis mainly pitched back (Fig. 8A *dotted line*) with a small roll component (Fig. 8B *dotted line*). Thus, the axis was ca.–90° relative to the heading. Head pitch was small during this initial period (Fig. 8A *solid line*), but head roll of ca.5° anticipated the roll component of the GIA (Fig. 8B). There was a sustained roll head component during the first 80% of the turning cycle, but the pitch head component remained small (<1.5°; Fig. 8B). During the last 40% of the turn, the GIA reached tilt angles of 20° (Fig. 8B), while the head roll tilt was maintained at 7° (Fig. 8B). Thus, the head roll led the roll component of the GIA tilt over most of the turn, and had the same magnitude, while the pitch component was sig-

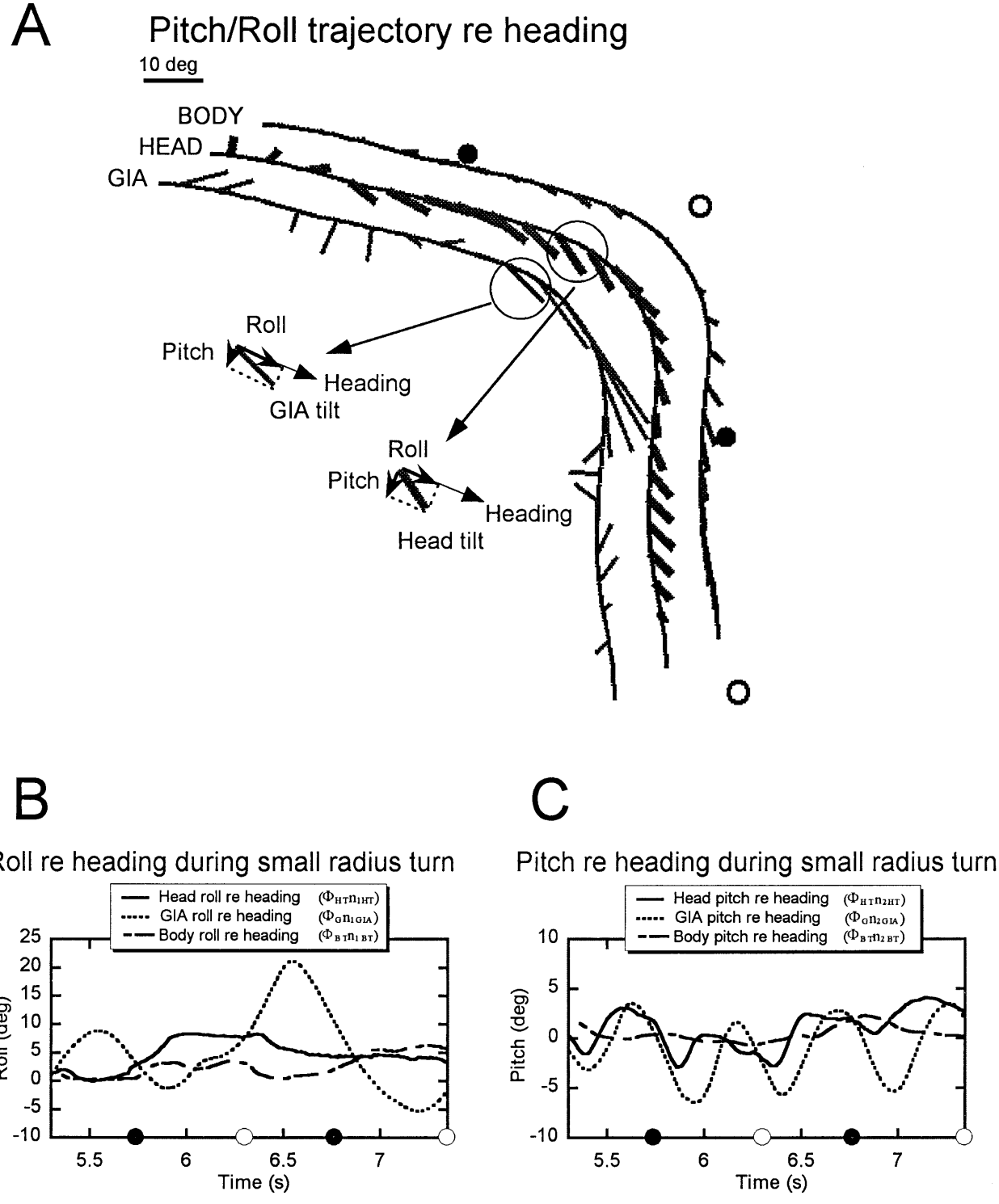

Fig. 7A–C Head, body, and GIA tilt data from a typical subject during turning. **A** Head, body, and GIA tilt axis during 50-cm radii turn. During the turn, the axes of GIA, head, and body tilt were aligned. **B** When executing these small-radius turns, there was sustained GIA roll ($\Phi_G n_{1GIA}$), body roll ($\Phi_{BT} n_{1BT}$), and head roll ($\Phi_{HT} n_{1HT}$) re heading. **C** There were small head pitch oscillations at approximately 2.0 Hz as during straight walking. Body pitch oscillations were negligible

nificantly reduced. The body pitch and roll was approximately that of the head, but with smaller amplitude. When subjects made turns of 200 cm, the GIA amplitude for pitch was approximately that during straight walking, but the roll component was significantly larger, reaching angles of 15° (Fig. 8E). Head and body tilts for both pitch and roll components were essentially those found during straight walking (Fig. 8F), but tilts of the head were always deviated inside the turn.

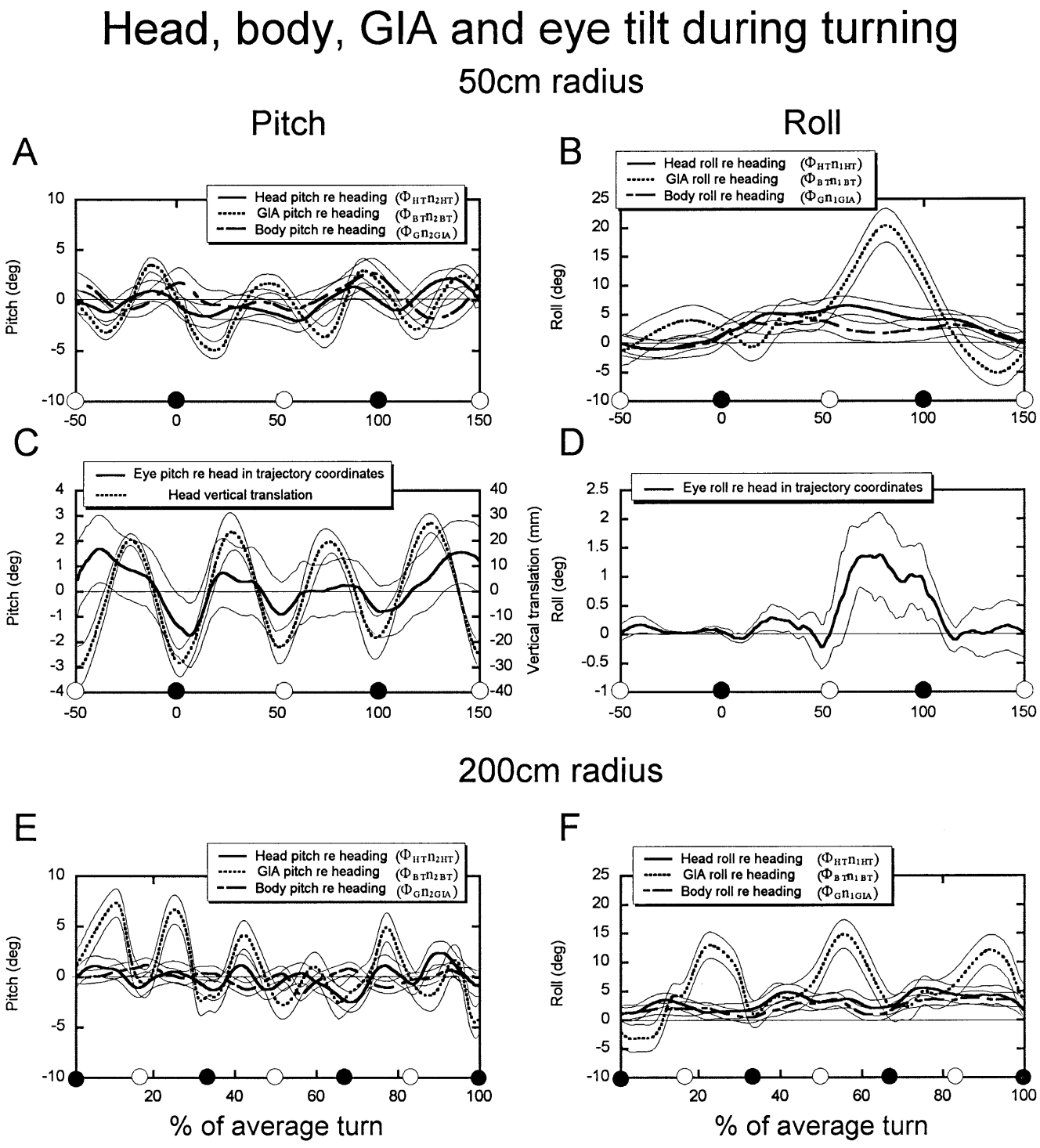

Fig. 8A–F Averaged data for five subjects while turning. **A** Head pitch re heading ($\Phi_{HT}n_{2HT}$), body pitch re heading ($\Phi_{BT}n_{2BT}$), and GIA pitch re heading ($\Phi_{G}n_{2GIA}$) during small-radii turn. When executing small-radius turns, there were GIA pitch oscillations at approximately 2.0 Hz. There were also negligible head and body pitch oscillations. **B** Head roll re heading ($\Phi_{HT}n_{2HT}$), body roll re heading ($\Phi_{BT}n_{1BT}$), and GIA roll re heading ($\Phi_{G}n_{1GIA}$) during small-radii turn. There was sustained head, body, and GIA roll about the heading during the turn. **C** Eye pitch re head in trajectory coordinates and head vertical translation. There were vertical pitch eye movements of about ±1° that oscillated with the step frequency. These movements were in phase with and compensated for vertical translation of the head during turning (0–100%). **D** Eye roll re head in trajectory coordinates. The duration of the roll closely approximated the duration of the tilt of the GIA. **E** Head pitch re heading ($\Phi_{HT}n_{2HT}$), body pitch re heading ($\Phi_{BT}n_{2BT}$), and GIA pitch re heading ($\Phi_{G}n_{2GIA}$) during large-radii turn. During large-radius turns, there are head, body, and GIA pitch oscillations at approximately 2.0 Hz similar to straight walking. **F** Head roll re heading ($\Phi_{HT}n_{2HT}$), body roll re heading ($\Phi_{BT}n_{1BT}$), and GIA roll re heading ($\Phi_{G}n_{1GIA}$) during large-radii turn. While there is an average sustained roll of head, body, and GIA during the execution of the turn, head, body, and GIA roll were more transient reaching peaks and then declining

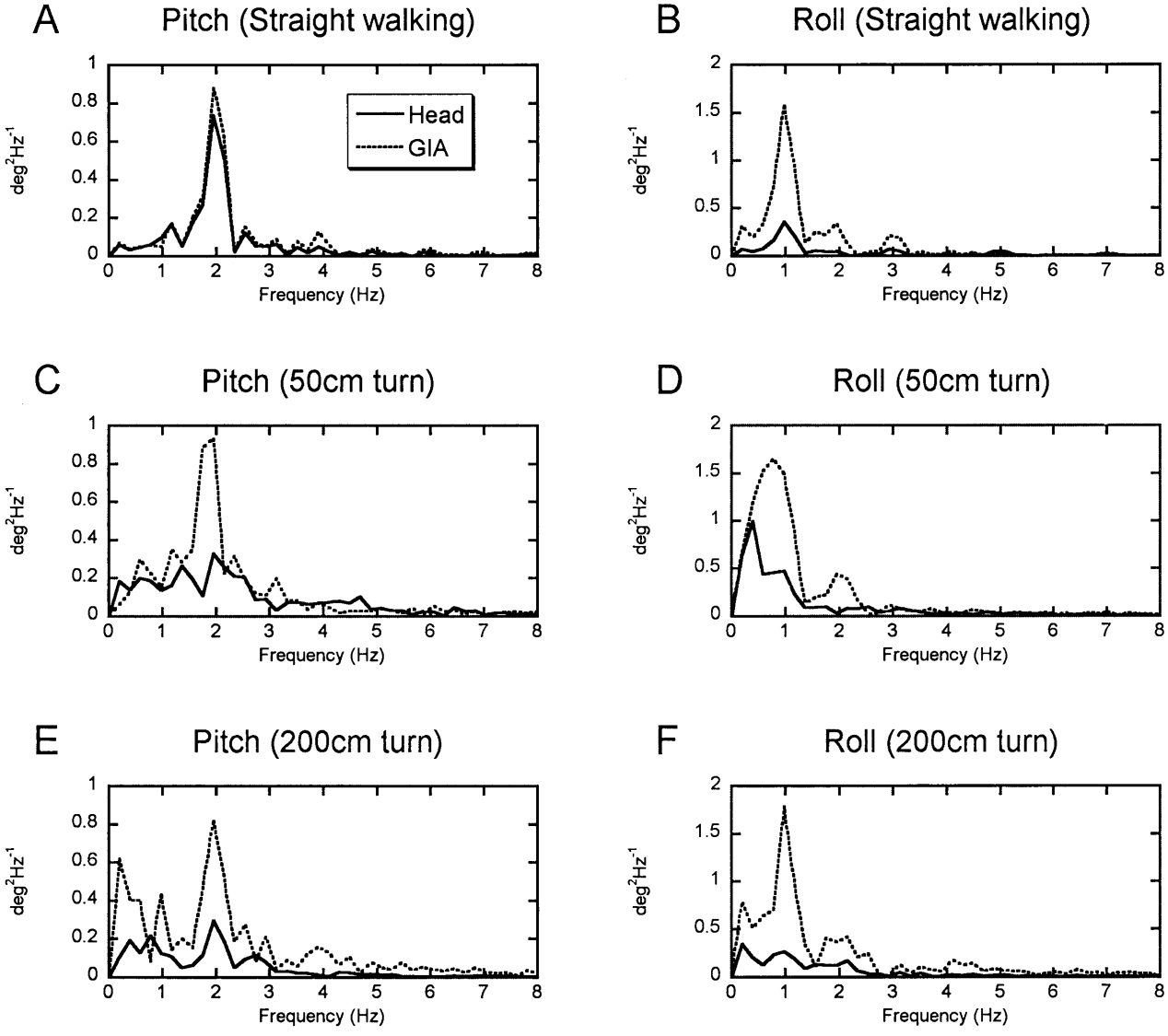

Fig. 9 Spectral content of GIA and head pitch and roll during straight walking (**A, B**), during turning over a 50-cm radius (**C, D**), and during turning over a 200-cm radius (**E, F**). During straight walking, the power spectra of the GIA and head pitch relative to the heading both peaked at 1 Hz, and the power spectra of the GIA and head roll both peaked at 2 Hz. During turning, the power spectra for both the GIA and head pitch had relatively larger components in the low frequency range, although there were still peaks at 2 Hz. Roll components had significant shifts to lower frequencies, with the bulk of the power being below 1 Hz

Spectral analysis of pitch and roll of the GIA and head were consistent with the differences between the pitch and roll components during straight walking and turning (Fig. 9). During straight walking (Fig. 9A, B), the power spectrum of the pitch of the GIA and head had peaks at 2 Hz and the power spectra were almost identical (Fig. 9A). The power spectra of the GIA and head roll relative to the heading both peaked at 1 Hz and had the same frequency behavior, although the GIA spectrum had much greater power (Fig. 9B). During turning, the power spectra for both the GIA and head pitch had relatively larger components in the low frequency range, although there were still local spectral maxima at 2 Hz (Fig. 9C). Roll components had significant shifts to lower frequencies, with the bulk of the power being below 1 Hz (Fig. 9D). As expected, the spectral components during turning over a 200-cm radius were a mixture of straight walking and turning. There were sharp peaks of pitch at 2 Hz (Fig. 9E) and roll at 1 Hz (Fig. 9F), although there were significant low frequency components for both pitch and roll (Fig. 9E, F).

Pitch and roll eye movements during turning

Despite the finding that the head did not oscillate in pitch more than 0.25° during turning (Fig. 8A), indicating insignificant activation of the compensatory aVOR, there were prominent vertical pitch eye movements of about ±1° that oscillated with the step frequency. These movements were compensatory for the vertical translation of the head (Fig. 8C), suggesting activation of the lVOR. The eyes also rolled relative to the head in trajectory coordinates in the *same direction* as the head roll (Fig. 8D). Thus, an orienting OCR response tended to align the eyes with the tilted GIA vector. The duration of the ocular torsion closely approximated the duration of the tilt of the GIA, and there was no anticipation of roll eye orientation. At the end of the turn (Fig. 8D; 100–150%), the head slowly rolled back to the upright position. The eyes reoriented to 0° following the GIA. The GIA then reversed although there was no ocular torsion as the subject walked straight ahead. For larger radius turns, the pulses in GIA were smaller (Fig. 8E, F) and the roll of the eyes was not consistent across all subjects. As yaw eye position led the heading, a positive roll component relative to the heading would point the optic axis down. Thus, during turns, alignment with the GIA pointed the optic axis toward looking into the turn and toward the floor, which would aid in navigating over uncertain terrain.

Discussion

The main findings of this study were that yaw, pitch, and roll movements of the body, head, and eyes maintain gaze in the direction of forward motion during straight walking and direct gaze in advance of the heading during turning. Grasso et al. (1996, 1998) showed that turns are anticipated by directing gaze about a yaw axis. Our results extend these findings and demonstrate that changes in the GIA are anticipated by tilting the head about the pitch and roll axes relative to heading. The results also show that the eyes are driven by tilts in the GIA during turning to help point gaze in the direction of turning. Finally, our results demonstrate that there are compensatory movements of the head and trunk during straight walking, and that orienting responses of the eyes, head, and body to tilts of the GIA play an important role in directing gaze during turning.

Eye, head, and body movements that stabilize gaze during forward locomotion and turning had both compensatory and orienting components. The pitch movements of the eyes that countered the vertical translation of the head during straight walking and turning are examples of compensatory responses, presumably from the lVOR. For example, during turning on a 50-cm radius, there was little angular pitch of the head (<0.5°), but the head moved vertically about 3.0 cm. In response, the eyes pitched (ca 0.5–1.0°) to compensate for the translation of the head (Fig. 8C) so that gaze pointed toward an approximately fixed point in space. This is consistent with previous studies in which the eye pitch response for close viewing distances was compensatory for vertical translation of the head and not with head pitch to maintain fixation on near targets (Moore et al. 1999). During turning about a 200-cm radius, there were elements of both straight walking and turning. Pitch eye movements were larger, and they were phase advanced relative to head vertical translation.

Ocular torsion into the direction of tilt during turning, particularly on a 50-cm radius (Fig. 8D), is an example of gaze orientation to the GIA. This is similar to the ocular counterrolling that occurs during static head tilts. In both cases, the torsion is into the direction of the linear acceleration and tends to align the yaw axis of the eye with the GIA. During turning on a 50-cm radius, the GIA tilted 20° relative to space, and the head rolled 7°. This would correspond to a static tilt of the head of 13° opposite to the direction of the GIA. In response, the eyes rolled an additional 1.0–1.5°, which corresponds well to the ocular counterrolling recorded in response to static head tilts of 13° (Dai et al. 1994; Diamond and Markham 1983; Diamond et al. 1979; Miller 1962). Parenthetically, it should be noted that the term ocular counterrolling may be a misnomer, since the eyes were rolling in the direction of head tilt. Since turning on a 50-cm radius is a common daily occurrence, ocular torsion in response to relative tilts between the head and the GIA, is likely to be functionally useful in directing gaze during locomotion. Eye velocity also orients toward a tilted GIA with respect to the head during steps of velocity through the velocity storage component of the aVOR (Dai et al. 1991; Raphan and Sturm 1991; Raphan et al. 1992; Wearne et al. 1999). No nystagmus occurred, however, either in pitch or roll during 50- or 200-cm turns in conjunction with the vigorous horizontal nystagmus observed during turning (Fig. 6). Thus, it is not clear that velocity storage, which generates orientation responses in humans with short latencies (Gizzi et al. 1994), was contributing to these responses. Such an analysis is beyond the scope of this paper.

One important question addressed by this study is to what extent orienting and compensatory responses affect the body and head movements during straight locomotion and during turning. Gaze stability during straight walking is maintained along the direction of forward motion of the body, despite relatively large oscillations and lateral displacements of the body in space. Throughout the trajectory, the body oscillates in space about the spatial yaw axis and shifts laterally. The head provides most of the compensation for these oscillations by counter-rotating in yaw so that the head stays within 1° from the straight-ahead position. This compensation maintains the head fixation distance (HFD) in the horizontal plane, in a manner analogous to maintenance of the HFD in the vertical plane during treadmill locomotion (Hirasaki et al. 1999; Moore et al. 1999). The aVOR also provides compensation so that the gaze in space varied less than a quarter of a degree on average over the stride cycle.

During straight walking, the head tilt axis had a predominant pitch component in the same direction as the GIA tilt, but the roll component of the head was 180° out of phase with the roll component of the GIA. The maximum roll occurred when the head was most lateral, pitch was zero, and yaw was a maximum. This orientation of the head would tend to maintain the head fixation point approximately invariant relative to the body. The frequency range of the head movement was approximately 1 Hz along yaw and roll axis, while close to 2 Hz along the pitch axis. Thus, the directions, phases, and frequency characteristics of head oscillations relative to the trajectory coordinate frame suggest that the yaw, pitch, and roll of the head during straight walking are compensatory lVCR responses for Y- and Z-axis translation rather than orientation responses to changes in the GIA.

In contrast to straight walking, turning motions had substantial orienting as well as compensatory head and gaze movements. The yaw rotation of the eyes in space led the head and body in the execution of the turn and orienting to the direction of motion with saccadic flicks. The slow phases compensated for the turning via the aVOR to maintain a constant angle in space while the quick phases moved gaze in anticipation of looking where subjects were going (Chun and Robinson 1978), steering the turn. The head also led the trajectory during the turn and steered smoothly in space. The body did not lead the trajectory and oscillated relative to the trajectory following the pattern during straight walking. Thus, while the movement of the legs and hips essentially governed the body, the head and eyes were governed by spatial maps, which directed the motion of the legs in a hierarchical control scheme, i.e., a top-down organization (Grasso et al. 1996; Pozzo et al. 1990). This control was directed toward maintaining the stability of gaze utilizing both compensatory and orienting components of movement. Since the body rotated relative to the stance feet during the turn, this too may have contributed in a bottom-up manner to the control of the head and eyes (Maurer et al. 1997; Mergner and Rosemeier 1998).

The roll orientations of the head during turning stand in sharp contrast to those during straight walking. There was almost exact alignment of the GIA and head roll axes during turning. GIA roll was anticipated by roll of the head. This anticipation may be necessary to overcome the head inertial response as a turn is initiated. This roll anticipation, together with anticipation in head yaw (Grasso et al. 1996), worked together to direct the turn and orient the head towards alignment with the GIA. Anticipation must be a property of active turning since no anticipation of tilt perception has been reported during passive generation of tilts on a linear sled or during centrifugation (Odkvist et al. 1996; Seidman et al. 1998). An inability of subjects to anticipate or rapidly compensate for the tilt of the GIA could be an explanation for the instability in gait when turning corners in patients with central vestibular and cerebellar disease. That is, the central vestibular system may not be able to generate appropriate head and body tilts to smoothly steer the turn.

There is no effective model of turning behavior as modeling of bipedal locomotion has been essentially confined to understanding locomotion as an optimization of energy consumption over the gait cycle (Alexander 1992; Minetti and Alexander 1997; Townsend and Seireg 1972; Townsend and Tsai 1976). The present study indicates that other constraints must be considered when modeling both straight and circular walking. That is, the central nervous system must generate appropriate signals to anticipate body heading and tilts of the GIA and generate appropriate head and eye movements to maintain stable gaze while optimizing energy consumption. The importance of gaze in determining the characteristics of locomotion have been emphasized previously (Grasso et al. 1996), suggesting that models which consider the head, arms, and trunk as a single unit during locomotion (Winter et al. 1993) must be expanded to include these considerations. An additional feature of turning which may be functionally important is the slowing down in body velocity as the turn is initiated, leading to a lower frequency content of head movement than during straight walking. Studies of the lVOR have shown that it has low frequency behavior (Telford et al. 1997, 1998), which can be associated with orientation responses such as ocular counterrolling (Wearne et al. 1999) and high frequency behavior (Paige and Tomko 1991), which compensates for equivalent high frequency head translation. If the VCR had similar orienting and compensatory behavior, where orientation would work better at lower frequencies, the slowing down could functionally improve the performance of orienting the head to align it with the GIA. Thus, while slowing may be a functional requirement as far as the feet are concerned, it may also aid head orientation by lowering the frequency components of head movement.

The body and head compensation about yaw and pitch during gait at an optimal velocity may be a property of bipedal locomotion, where there is considerable vertical and horizontal linear accelerations over the gait cycle (Hirasaki et al. 1999; Moore et al. 1999). This is because at an optimal walking speed the linear vertical distance traversed is 30–70 mm as the body shifts from double stance to single stance mode, with an oscillation frequency of close to 2.0 Hz (Hirasaki et al. 1999; Moore et al. 1999). This gives vertical accelerations in the range of 0.2–0.6 g (Hirasaki et al. 1999). While the accelerations in the lateral direction (ca 0.1 g) are smaller due to the lower frequencies of oscillation, gaze is maintained in the direction of forward motion. Studies of quadrupedal gait (Broton et al. 1996; Charteris et al. 1979; McMahon 1975; Schoner et al. 1990) have been confined to analysis of joint angles, and the movements of the body, head, and eyes have not been studied. Quadrupeds are supported by at least two limbs throughout the gait cycle (Howland et al. 1995; Lanyon and Smith 1970; Mori et al. 1996) and may consequently have altered vertical body and head traversals as well as compensatory responses compared to bipeds.

In summary, we have shown that there is close coordination between the oscillatory movements of the lower body that sustain bipedal locomotion, and the head and eye motions that direct and orient gaze with respect to the GIA. We suggest that compensatory and orienting movements produced by the VCR and VOR are important in mediating between the lower and upper body and in stabilizing gaze and posture.

Acknowledgements This study was supported by NIH grants DC03284, EY04148, and EY01867, NASA Cooperative Agreement NCC 9-58 with the National Space Biomedical Research Institute (NSBRI), NY State HEAT grant (CUNY), and PSC-CUNY Award 61394-30.

References

Alexander RM (1992) A model of bipedal locomotion on compliant legs. Philos Trans R Soc Lond B 338:189–198

Altmann SL (1986) Rotations, quaternions and double groups. Oxford University Press, New York

Andriacchi TP, Ogle JA, Galante JO (1977) Walking speed as a basis for normal and abnormal gait measurements. J Biomech 10:261–268

Bloomberg JJ, Peters BT, Smith SL, Huebner WP, Reschke MF (1997) Locomotor head-trunk coordination strategies following space flight. J Vestib Res 7:161–177

Broton JG, Nikolic Z, Suys S, Calancie B (1996) Kinematic analysis of limb position during quadrupedal locomotion in rats. J Neurotrauma 13:409–416

Cappozzo A (1981) Analysis of the linear displacement of the head and trunk during walking at different speeds. J Biomech 14:411–425

Charteris J, Leach D, Taves C (1979) Comparative kinematic analysis of bipedal and quadrupedal locomotion: a cyclographic technique. J Anat 128:803–819

Chun KS, Robinson DA (1978) A model of quick phase generation in the vestibuloocular reflex. Biol Cybern 28:209–221

Clement G, Reschke MF (1996) Neurosensory and sensory-motor functions, chapter 4. Springer, Berlin Heidelberg New York

Crane BT, Demer JL (1997) Human gaze stabilization during natural activities: translation, rotation, magnification, and target distance effects. J Neurophysiol 78:2129–2144

Dai M, Raphan T, Cohen B (1991) Spatial orientation of the vestibular system: dependence of optokinetic after nystagmus on gravity. J Neurophysiol 66:1422–1438

Dai M, McGarvie L, Kozlovskaya I, Raphan T, Cohen B (1994) Effects of spaceflight on ocular counterrolling and the spatial orientation of the vestibular system. Exp Brain Res 102:45–56

Diamond SG, Markham CH (1983) Ocular counterrolling as an indicator of vestibular otolith function. Neurology 33:1460–1469

Diamond SG, Markham CH, Simpson NE, Curthoys IS (1979) Binocular counterrolling in humans during dynamic rotation. Acta Otolaryngol (Stockh) 87:490–498

Fick A (1854) Die Bewegungen des menschlichen Augapfels. Z Rat Medizin 4:109–128

Gizzi M, Raphan T, Rudolph S, Cohen B (1994) Orientation of human optokinetic nystagmus to gravity: a model based approach. Exp Brain Res 99:347–360

Goldstein H (1980) Classical mechanics, 2nd edn. Addison-Wesley, Reading, Mass

Grasso R, Glasauer S, Takei Y, Berthoz A (1996) The predictive brain: anticipatory control of head direction for the steering of locomotion. Neuroreport 7:1170–1174

Grasso R, Prevost P, Ivanenko YP, Berthoz A (1998) Eye-head coordination for the steering of locomotion in humans: an anticipatory synergy. Neurosci Lett 253:115–118

Grossman GE, Leigh RJ (1990) Instability of gaze during locomotion in patients with deficient vestibular function. Ann Neurol 27:528–532

Haustein W (1989) Consideration on Listing's law and the primary position by means of a matrix description of eye position control. Biol Cybern 60:411–420

Hirasaki E, Moore ST, Raphan T, Cohen B (1999) Effects of walking velocity on vertical head and body movements during locomotion. Exp Brain Res 127:117–130

Howland DR, Bregman BS, Goldberger ME (1995) The development of quadrupedal locomotion in the kitten. Exp Neurol 135:93–107

Imai T, Hirasaki E, Moore ST, Raphan T, Cohen B (1998) Stabilization of gaze when turning corners during overground walking. Soc Neurosci Abstr 24:415

Imai T, Takeda N, Morita M, Koizuka I, Kubo T, Miura K, Nakamae K, Fujioka H (1999) Rotation vector analysis of eye movement in three dimensions with an infrared CCD camera. Acta Otolaryngol (Stockh) 119:24–28

Inman VT (1966) Human locomotion. Can Med Assoc J 94: 1047–1054

Inman VT, Ralston H, Todd F (1981) Human walking. Williams and Williams, Baltimore

Ito S, Odahara S, Hiraki M, Idate M (1995) Evaluation of imbalance of the vestibulo-spinal reflex by "the circular walking test.". Acta Otolaryngol (Stockh) Suppl 519:124–126

Lanyon LE, Smith RN (1970) Bone strain in the tibia during normal quadrupedal locomotion. Acta Orthop Scand 41:238–248

Maurer C, Kimmig H, Trefzer A, Mergner T (1997) Visual object localization through vestibular and neck inputs. 1. Localization with respect to space and relative to the head and trunk mid-sagittal planes. J Vestib Res 7:119–135

McMahon TA (1975) Using body size to understand the structural design of animals: quadrupedal locomotion. J Appl Physiol 39:619–627

Mergner T, Rosemeier T (1998) Interaction of vestibular, somatosensory, and visual signals for postural control and motion perception under terrestrial and microgravity conditions – a conceptual model. Brain Res Rev 28:118–135

Miller EF II (1962) Counterrolling of the human eyes produced by head tilt with respect to gravity. Acta Otolaryngol (Stockh) 54:479–501

Minetti AE, Alexander RM (1997) A theory of metabolic costs for bipedal gait. J Theor Biol 186:467–476

Moore ST, Hirasaki E, Raphan T, Cohen B (1997) Effective rotation axes (ERA) during voluntary pitch and yaw head movements. Soc Neurosci Abstr 23:753

Moore ST, Hirasaki E, Cohen B, Raphan T (1999) Effect of viewing distance on the generation of vertical eye movements during locomotion. Exp Brain Res 129:347–361

Mori S, Miyashita E, Nakajima K, Asano M (1996) Quadrupedal locomotor movements in monkeys (*M. fuscata*) on a treadmill: kinematic analysis. Neuroreport 7:2277–2285

Murray MP, Kory RC, Clarkson BH, Sepic SB (1966) Comparison of free and fast speed walking patterns of normal men. Am J Phys Med 45:8–24

Odkvist LM, Gripmark MA, Larsby B, Ledin T (1996) The subjective horizontal in eccentric rotation influenced by peripheral vestibular lesion. Acta Otolaryngol (Stockh) 116:181–184

Paige GD (1989) The influence of target distance on eye movement responses during vertical linear motion. Exp Brain Res 77:585–593

Paige GD, Tomko DL (1991) Eye movement responses to linear head motion in the squirrel monkey. II. Visual-vestibular interactions and kinematic considerations. J Neurophysiol 65:1183–1196

Pozzo T, Berthoz A, Lefort L (1990) Head stabilization during various locomotor tasks in humans. I. Normal subjects. Exp Brain Res 82:97–106

Pozzo T, Berthoz A, Lefort L, Vitte E (1991) Head stabilization during various locomotor tasks in humans. II. Patients with bilateral peripheral vestibular deficits. Exp Brain Res 85:208–217

Raphan T (1998) Modeling control of eye orientation in three dimensions. I. Role of muscle pulleys in determining saccadic trajectory. J Neurophysiol 79:2653–2667

Raphan T, Cohen B (1996) How does the vestibulo-ocular reflex work? In: Baloh RW, Halmagyi GM (eds) Disorders of the vestibular system. Oxford University Press, New York, pp 20–47

Raphan T, Sturm D (1991) Modeling the spatiotemporal organization of velocity storage in the vestibuloocular reflex by optokinetic studies. J Neurophysiol 66:1410–1420

Raphan T, Dai M, Cohen B (1992) Spatial orientation of the vestibular system. Ann NY Acad Sci 656:140–157

Raphan T, Wearne S, Cohen B (1996) Modeling the organization of the linear and angular vestibulo-ocular reflexes. Ann NY Acad Sci 781:348–363

Rodriguez O (1840) Des lois geometriques qui regissent les desplacements d'un systeme solide dans l'espace et de la variation des coordonnees provenant de deplacements consideres independamment des causes qui peuvent les produire. J Mathematiques Pures Appliquees 5:380–440

Schnabolk C, Raphan T (1994) Modeling three dimensional velocity-to-position transformation in oculomotor control. J Neurophysiol 71:623–638

Schoner G, Jiang WY, Kelso JA (1990) A synergetic theory of quadrupedal gaits and gait transitions. J Theor Biol 142:359–391

Schwarz C, Miles FA (1991) Ocular responses to translation and their dependence on viewing distance. I. Motion of the observer. J Neurophysiol 66:851–864

Seidman SH, Telford L, Paige GD (1998) Tilt perception during dynamic linear acceleration. Exp Brain Res 119:307–314

Takahashi M (1990) Head stability and gaze during vertical whole-body oscillations. Ann Otol Rhinol Laryngol 99:883–888

Telford L, Seidman SH, Paige GD (1997) Dynamics of squirrel monkey linear vestibuloocular reflex and interactions with fixation distance. J Neurophysiol 78:1775–1790

Telford L, Seidman SH, Paige GD (1998) Canal-otolith interactions in the squirrel monkey vestibulo-ocular reflex and the influence of fixation distance. Exp Brain Res 118:115–125

Townsend MA, Seireg A (1972) The synthesis of bipedal locomotion. J Biomech 5:71–83

Townsend MA, Tsai TC (1976) Biomechanics and modeling of bipedal climbing and descending. J Biomech 9:227–239

Tweed D, Cadera W, Vilis T (1990) Computing three-dimensional eye position quaternions and eye velocity from search coil signals. Vision Res 30:97–110

Tweed D, Misslisch H, Fetter M (1994) Testing models of the oculomotor velocity-to-position transformation. J Neurophysiol 72:1425–1429

Wearne S, Raphan T, Cohen B (1999) Effects of tilt of the gravito-inertial acceleration vector on the angular vestibuloocular reflex during centrifugation. J Neurophysiol 81:2175–2190

Winter DA, MacKinnon CD, Ruder GK, Wieman C (1993) An integrated EMG/biomechanical model of upper body balance and posture during human gait. In: Allum JMJ, Allum-Macklenburg DJ, Harris FP, Prohst R (eds) Progress in brain research. Elsevier, Amsterdam, pp 359–367